Resonant Excitation of Graphene *K*-Phonon and Intra-Landau-Level Excitons in Magneto-Optical Spectroscopy

M. Orlita,[1,2] Liang Z. Tan,[3] M. Potemski,[1] M. Sprinkle,[4] C. Berger,[4,5] W. A. de Heer,[4] Steven G. Louie,[3,*] and G. Martinez[1]

[1]*Laboratoire National des Champs Magntiques Intenses, CNRS-UJF-UPS-INSA, B.P. 166, 38042 Grenoble Cedex 9, France*

[2]*Institute of Physics, Charles University, Ke Karlovu 5, CZ-121 16 Praha 2, Czech Republic*

[3]*Department of Physics, University of California at Berkeley, and Materials Sciences Division, Lawrence Berkeley National Laboratory, Berkeley, California, 94720, USA*

[4]*School of Physics, Georgia Institute of Technology, Atlanta, Georgia 30332, USA*

[5]*Institut Néel, CNRS-UJF B.P. 166, 38042 Grenoble Cedex 9, France*

(Received 15 January 2012; published 13 June 2012; publisher error corrected 15 June 2012)

Precise infrared magnetotransmission experiments have been performed in magnetic fields up to 32 T on a series of multilayer epitaxial graphene samples. We observe changes in the spectral features and broadening of the main cyclotron transition when the incoming photon energy is in resonance with the lowest Landau level separation and the energy of a *K* point optical phonon. We have developed a theory that explains and quantitatively reproduces the frequency and magnetic field dependence of the phenomenon as the absorption of a photon together with the simultaneous creation of an intervalley, intra-Landau-level exciton, and a *K* phonon.

DOI: 10.1103/PhysRevLett.108.247401 PACS numbers: 78.67.Wj, 73.22.Pr, 78.20.Ls

Phonons, electrons, holes, and plasmons are fundamental elementary excitations in solids, and their interactions among themselves and with light strongly influence the electronic and optical properties of a system. Graphene, a single atomic layer of carbon, exhibits many fascinating properties of basic and practical interest. Its low-energy charge carriers behave like two-dimensional (2D) massless Dirac fermions. The unique electronic structure of graphene has led to the prediction and observation of a number of novel phenomena involving various multiple elementary excitation interactions including electron-photon, electron-phonon, electron-electron, and electron-plasmon couplings. Recent discoveries include the observation of plasmarons in angle-resolved photoemission spectroscopy [1], controlling of quantum pathways in inelastic light scattering [2], and strong excitonic effects in optical absorption [3–5], among others.

In this Letter, we report the discovery of another intriguing phenomenon seen in the magneto-optical response of graphene when the incoming photon energy is in resonance with the lowest Landau-level separation and the energy of a Brillouin zone boundary phonon at the *K* point. The frequency and magnetic field dependence of the spectral features are understood and explained in terms of resonant transitions which involve the absorption of a photon together with the simultaneous creation of an intervalley, intra-Landau level exciton, and a *K* phonon. The phenomenon provides a novel manifestation of multiple elementary excitation interactions in condensed matter.

The phonons that interact the most strongly with electrons in graphene are those at the Brillouin zone center (Γ) and at the Brillouin zone boundary (*K*) [6,7]. The Γ phonon has been the subject of theoretical study [8] and its signatures have been observed in several experiments [9,10]. The *K* phonon also interacts strongly with electrons, giving rise to characteristic features in Raman spectra [10]. Compared to Γ phonons, the effect of *K* phonons on optical experiments is more subtle and indirect, due to the large difference in momenta between photons and the *K* phonons. The large wave vector of the *K* phonons may also couple the two inequivalent valleys in the graphene band structure, introducing an additional degree of freedom into the system. The present study shows that this valley degree of freedom in the coupling has unique and important consequences in the magneto-optical response of graphene.

In our experiment, precise infrared transmission measurements were performed on multilayer epitaxial graphene samples, at 1.8 K, under magnetic fields up to 32 T. It is known that under a perpendicular magnetic field *B*, the electronic structure of graphene is quantized to discrete Landau levels (LL) with the energy $E_n = \mathrm{sgn}(n) v_F \sqrt{2e\hbar B|n|}$ where n are integers including 0. Multiple optical transitions are allowed and have been observed [11] between LL $|n|$ to $|n| \pm 1$ if these levels have appropriate occupation factors. We focus our attention on the magnetic field evolution of the transmission spectrum near the main optical absorption peak, with energy $E_{01} = v_F \sqrt{2e\hbar B}$ involving the $n = 0$ LL (i.e., transitions from $n = -1$ to $n = 0$ or from $n = 0$ to $n = 1$.) It is discovered that a strong change in the optical spectrum occurs when E_{01} reaches an energy near the energy of a *K* phonon. This is interpreted as a signature of a new multiple elementary excitation phenomenon involving interaction between electrons and the *K* phonon, and a theory is developed to explain quantitatively the phenomenon.

A series of four multilayer epitaxial graphene samples were grown [12] on the C-terminated surface of SiC. The thickness of the SiC substrate has been reduced to 60 μm in order to minimize the very strong double phonon absorption of SiC in the energy range of interest. Whereas the transmission spectra reveal some contributions of graphite Bernal stacked inclusions, the major part displays the electronic band structure of an isolated graphene monolayer resulting from the characteristic rotational stacking of the sheets [13]. Using standard techniques [14], we measure the relative transmission spectra $\mathrm{TR}(B, \omega)$ (Supplemental Material, Sec. I [15]).

The TR spectra of the sample $S1$ are displayed in Figs. 1(a) and 1(b) for different values of B. They show, as for all samples, an apparent splitting of the transmission dip into two and a pronounced increase of the broadening of the dip, as well as a change in the B-field dependence of the overall position E_{01} for fields larger than 17 T.

In general, the detailed analysis of such spectra requires the use of a multilayer dielectric model including all layer dielectric properties of the sample. In particular, for each graphene sheet, one has to introduce the corresponding components of the optical conductivity tensor $\sigma_{xx}(\omega)$ and $\sigma_{xy}(\omega)$, defined by $J_\alpha = \sum_\beta \sigma_{\alpha\beta}\mathcal{E}_\beta$ (J_α and $\mathcal{E}_\beta$ denote current density and electric field vectors, respectively). Here, the x and y-axis lie in the plane of the sample. For instance, $\sigma_{xx}(\omega)$, for transitions involving the $n = 0$ LL, is written as:

$$\sigma_{xx}(\omega, B) = \imath \frac{e^3 B}{h\omega} \sum_{r,s} \frac{M_{r,s}^2 [f_r(B) - f_s(B)]}{\hbar\omega - E_{r,s}(B) + \imath\Gamma_{rs}(B)}, \quad (1)$$

where r, s scan the values 0 and ± 1, $0 \leq f_r \leq 1$ is the occupation factor of the LL r, $M_{r,s}$ the optical matrix element, $E_{r,s} = E_r - E_s = E_{01}$ and $\Gamma_{rs}(B) = \Gamma_{01}(B)$ measures the broadening of the transition . However, this approach requires the knowledge of the number of effective active layers as well as their carrier densities which, in turn, implies some approximations (Supplemental Material, Sec. II [15]). We will use this approach in a refined analysis, but in our initial analysis, fit directly the E_{01} transition with a single Lorentzian line.

This fit provides, for each value of B, two independent parameters $E_{01}(B)$ and $\Gamma_{01}(B)$ which are plotted in Fig. 1(c) as a function of $B^{1/2}$. The variation of $\Gamma_{01}(B)$ shows clearly an extra bump beyond 17 T [clearly apparent in Fig. 1(b)] whereas, that of $E_{01}(B)/B^{1/2}$ exhibits a downwards kink at the same field. The evolution of $\Gamma_{01}(B)$ is decomposed in two parts: one named $\gamma_{01}(\mathrm{meV}) = 2.3 + 0.6\sqrt{B} + 0.24B$ (full dots) and an extra contribution to Γ_{01} represented by stars in the top panel of Fig. 1(c). The same decomposition is obtained for all samples with slightly different coefficients which are discussed in the Supplemental Material, Sec. II [15]. The $\sqrt{B}$ dependence of γ_{01} is attributed to scattering with short range impurities [16]; the linear variation with B is not predicted by scattering mechanisms considered in previous studies [16] and will be discussed later. The shape of the extra contribution to Γ_{01} has a threshold at around 17 T ($\sim$ 151 meV) with a maximum amplitude of about 2 meV for all samples, within the experimental uncertainties, before decreasing at higher fields. In that energy range, the only likely excitations in graphene which could play a role are the zone boundary K phonons [17,18]. Note that, at this threshold energy, the evolution $E_{01}/B^{1/2}$ [bottom panel of Fig. 1(c)] is the signature of interactions because, in the absence of such interactions, it should be an horizontal line. This is reminiscent of the response function of the Fröhlich interaction observed in polar semiconductors [14,19], where a zone center

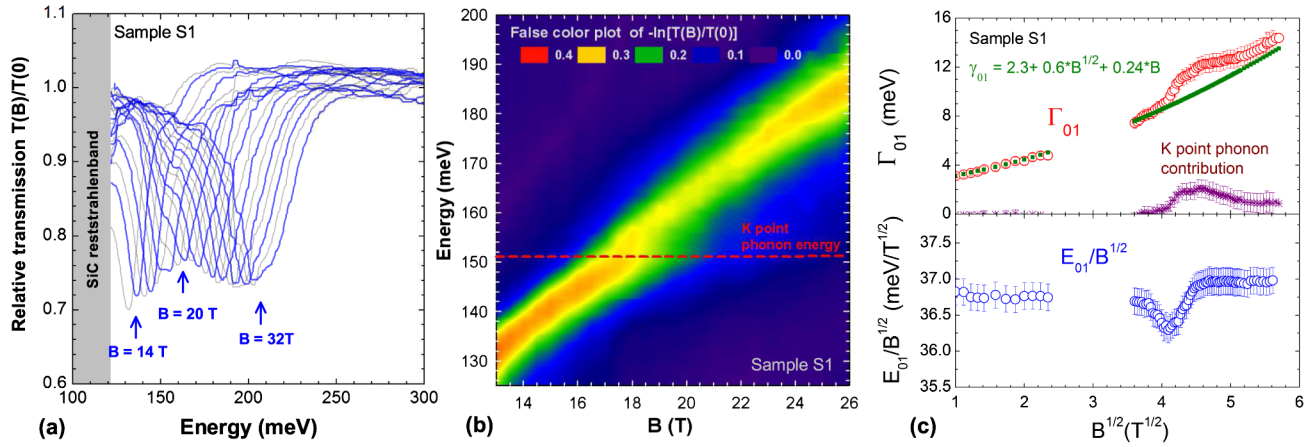

FIG. 1 (color online). (a) Relative transmission spectra $(T(B)/T(0))$ of sample $S1$, for different magnetic field values. (b) Same data as in (a) presented in a false color plot of $-\ln[T(B)/T(0)]$. (c) Bottom panel: variation of cyclotron transition energy $E_{01}/B^{1/2}$ as a function of $B^{1/2}$ (open circles). Top panel: variation of the fitted linewidth $\Gamma_{10}(B)$ of the transition $E_{01}(B)$ as a function of $B^{1/2}$ (open circles). This variation is de-convoluted is two parts, one named $\gamma_{01}(B)$ (solid dots) and the remaining part (stars) which is assigned to the K phonon contribution.

longitudinal optical phonon is emitted when the energy of the cyclotron transition exceeds that of the phonon. However, graphene is not a polar material and, furthermore, we are not expecting a direct interaction of the K phonon with the infrared light. One therefore has to explain why and how the K phonons enter the interaction.

The mechanism for the interaction of the cyclotron transition with the K phonon is not *a priori* clear for the reason of conservation of wave vector, in other words, a state corresponding to an optical cyclotron transition which has wave vector 0 cannot decay into a state with a phonon of wave vector $\vec{K}$ without simultaneously emitting another entity of wave vector $-\vec{K}$. Given that this interaction must necessarily involve the electron-phonon interaction, and that the low-energy electronic states at the two valleys of graphene are separated in reciprocal space by a wave vector $\vec{K}$, we propose that an intervalley intra-LL electron scattering process (creation of a zero-energy intervalley electron-hole pair) is responsible for the observed phenomenon (Fig. 2).

To explain the observed spectral features, we shall consider the coupling of the photoexcited (cyclotron transition) states (denoted as $|\eta_1(j,k)\rangle$ and $|\eta_2(j,k)\rangle$ for the $0 \rightarrow 1$ and $-1 \rightarrow 0$ LL transitions, respectively) with an excited state of the system containing an intervalley, intra-Landau-level electron-hole pair excitation and a K phonon of wave vector $\vec{K}+\vec{q}$ (denoted as $|\xi_{\vec{q}}(j,k)\rangle$). See Fig. 2. Here j is the valley index and k is the quantum number which describes the degenerate states within a LL. As illustrated in Fig. 2, at cyclotron transition energy E_{01} near $\hbar\omega_{\vec{K}+\vec{q}}$, $|\eta_1(j,k)\rangle$ and $|\eta_2(j,k)\rangle$ are connected to $|\xi_{\vec{q}}(j,k)\rangle$ via an emission of $\vec{K}+\vec{q}$ phonons. The electron-phonon coupling in the system can then strongly mix these states at resonance and lead to significant changes in the absorption spectrum.

In order to reproduce quantitatively the transmission spectra, one has now to use the multilayer dielectric model (Supplemental Material, Sec. II [15]). The optical conductivity is calculated using the Green's function formalism introduced by Toyozawa [20]. The conductivity components are

$$\mathrm{Re}\sigma_{ij}(\hbar\omega) \propto \mathrm{Im}\langle 0|M_i G(\hbar\omega) M_j|0\rangle, \qquad (2)$$

where $|0\rangle$ is the ground state of the system, and M_i, M_j are row and column vectors containing optical matrix elements. G is the retarded Green's function written here as $G(\hbar\omega) = [\hbar\omega - H - \Sigma(\omega) + is]^{-1}$ with $s \rightarrow 0^-$ with H being a 3×3 Hamiltonian describing the interaction between the three states $|\eta_1\rangle$, $|\eta_2\rangle$ and $|\xi\rangle$. The poles of G are broadened by a self energy $\Sigma(\omega)$ reflecting additional lifetime effects due to the K phonon dispersion and the excitations from electron-acoustic phonons scattering, electron-electron interactions, and other environmental effects not captured by H (Supplemental Material, Sec. V [15]). In the theoretical calculations, we have incorporated

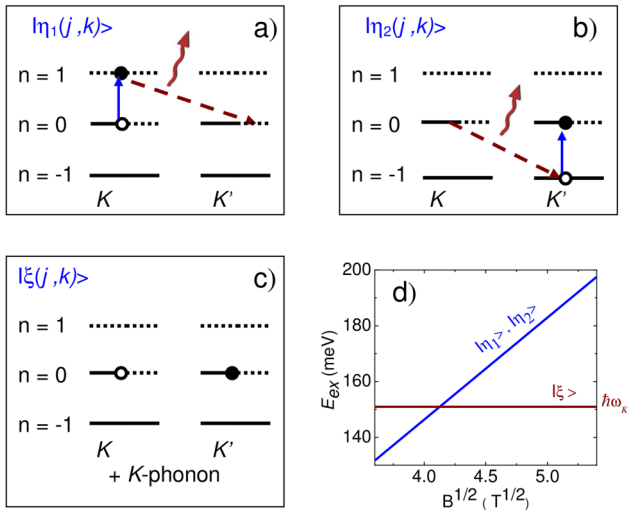

FIG. 2 (color online). Cyclotron resonant excitations $|\eta_1(j,k)\rangle$ (a) and $|\eta_2(j,k)\rangle$ (b) involving the $n=0$ Landau levels, at either the K or K' valley, with the excitation energy $E_{\mathrm{ex}} = E_{01}$. (c) Excited state $|\xi_{\vec{q}}(j,k)\rangle$ corresponding to intervalley transfer of an electron within the $n=0$ LL from $\vec{K}$ to $\vec{K}'$ and creation of a phonon with wave vector $\vec{K}+\vec{q}$, which has excitation energy $E_{\mathrm{ex}} = \hbar\omega_{\vec{K}+\vec{q}}$. (d) At resonance, i.e., $E_{01} = \hbar\omega_{\vec{K}+\vec{q}}$, $|\eta_1\rangle$ and $|\eta_2\rangle$ may be transformed to $|\xi\rangle$ via an emission of a $\vec{K}+\vec{q}$ phonon as indicated by the dashed brown lines. The mixing between the three excited states, mediated by the electron-phonon interaction, is the strongest when the resonance condition is satisfied ($E_{01} = \hbar\omega_{\vec{K}+\vec{q}}$). Electron-phonon scatterings involving LL $|n| \geq 2$ do not result in similar resonances in the experimental energy range (Supplemental Material, Sec. IV [15]). In general, there are scattering processes involving phonons of different $\vec{q}$ vectors near K, but we find the coupling strength significant only in a small region with $\vec{q} \approx 0$ where the phonon energy is essentially constant and equal to $\hbar\omega_K$. The theoretical description of this continuum of near K phonons may be incorporated effectively by considering a single state $|\xi\rangle$ with a complex self-energy and using an appropriately renormalized coupling constant between $|\eta_1\rangle$, $|\eta_2\rangle$ and $|\xi\rangle$ (see derivation in the Supplemental Material, Sec. IV [15]).

this additional physics near resonance with a broadening function of the form $\Gamma_{01}(\omega, B) = \gamma_{01}(B) + \mathrm{Im}[\Sigma(\omega)]$ with $\gamma_{01}(B)$ given above and $\mathrm{Im}(\Sigma)$ taken to be $\mathrm{Im}[\Sigma(\omega)] = \pi A^2 f(R/\hbar\omega_K)\theta(\hbar\omega - \hbar\omega_K)e^{-R(\omega/\omega_K - 1)}$. The derivation of the form of $\mathrm{Im}[\Sigma(\omega)]$ within our theoretical model is given in the Supplemental Material, Secs. IV and V [15]. $A^2(\mathrm{meV}^2) = 1.94 \times B(\mathrm{T})$ is the electron-phonon parameter determined from Ref. [18]. f is a factor, dependent on the relative magnitudes of the valley (Δ_V) and spin (Δ_S) spittings of the $n=0$ LL, that is determined by the occupations of the spin and valley sublevels of the $n=0$ LL (Supplemental Material, Sec. IV [15]). The threshold structure of $\mathrm{Im}[\Sigma(\omega)]$ represents the onset of K phonon emission at energies above $\hbar\omega_K$. The only parameters in the theory are the phonon energy $\hbar\omega_K$ and the factor R. The absorption spectra can be obtained from $\mathrm{Re}\sigma(\omega)$ by a

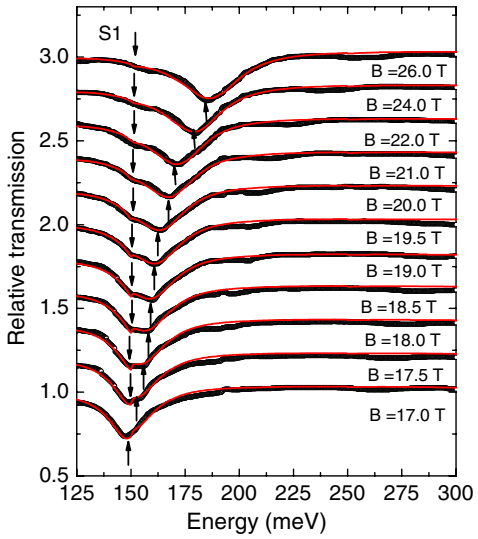

FIG. 3 (color online). Comparison, for different values of the magnetic field, of experimental data for sample $S1$ (open black dots) with the theoretical curves (red lines) using the proposed K phonon interaction model. As a guide for the eye, upward arrows show the evolution of the main cyclotron resonance line whereas downward arrows point the structure corresponding to the emission of K phonons.

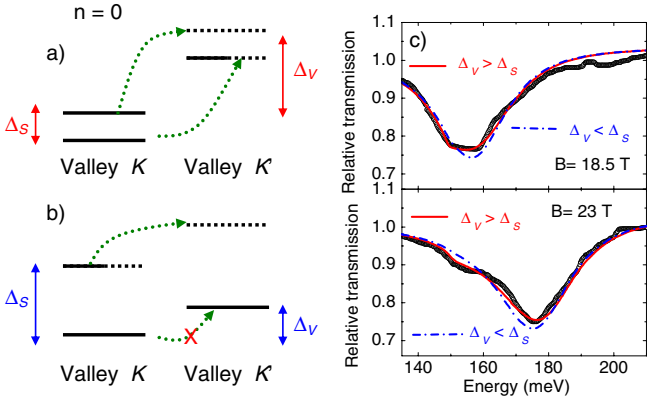

FIG. 4 (color online). (a), (b) The spin and valley sublevels of the $n = 0$ LL, for the case when $\Delta_V > \Delta_S$ and $\Delta_V < \Delta_S$ respectively. In the former case, intervalley electronic transitions are possible for both spin orientations. In the latter case, only one spin orientation supports intervalley electronic transitions, owing to the Fermi factor. The effective coupling strength is therefore different in the two cases giving rise to different predictions for the transmission spectra. (c) A comparison between experimental spectra and theoretical simulations for $\Delta_V > \Delta_S$ and $\Delta_V < \Delta_S$ for values of magnetic field $B = 18.5$ T and $B = 23.0$ T respectively. For all our samples the splitting of the valley degeneracy is larger than the spin splitting. This is consistent with recent tunneling spectroscopy experiments on graphene on SiC [27]. Theoretical discussions on the relative magnitudes of these splittings can be found in Refs. [21–24,28,29].

simple proportionality relation (Supplemental Material, Sec. V [15] and Ref. [11]).

In Fig. 3, we compare the experimental data, for sample $S1$, with the calculated results from the model with $\Delta_V > \Delta_S$. We have taken $\hbar\omega_K = 151$ meV and $R = 3$. The Fermi velocity $v_{F01} = 1.012 \times 10^6$ ms^{-1} for the transitions between the $n = 0$ LL and $n = \pm 1$ LL has been determined experimentally from the positions of the cyclotron transition lines (Supplemental Material, Secs. II and III [15]). The same parameters have been used for all the graphene samples (Supplemental Material, Sec. III [15]). The good agreement between theory and experiment, for all samples, lends strong support to the physical mechanism proposed for the phenomenon. It is, however, only obtained when assuming $\Delta_V > \Delta_S$ (Fig. 4).

An interpretation of the linear term in $\gamma_{01}(B)$ is that it may be a broadening resulting from the breaking of the valley degeneracy (Fig. 4), consistent with the prediction that $\Delta_V \propto B$, according to several theoretical models [21–23]. In this picture, the values of E_{01} at the two valleys differ by Δ_V [24], resulting in a broadening of the main line by a similar amount. An inspection of the linear term in $\gamma_{01}(B)$ shows that it is greater than the value of Δ_S due to Zeeman splitting. This is consistent with our conclusion that $\Delta_V > \Delta_S$ in our samples (Fig. 4). However, further investigations are needed to test if the valley splitting is indeed the main contributor to the linear term in γ_{01}.

To conclude, we have observed splitting of spectral features and broadening of the main absorption line above 17 T in our infrared transmission experiments on epitaxial graphene that we attribute to a resonance between cyclotron transitions and K phonon emission coupled with a zero-energy intervalley electron-hole excitation. We have developed a theoretical model that reproduces the experimental results with quantitative agreement, thereby shedding light on the nature of the optical transitions and electron-phonon interaction in graphene under strong magnetic fields. Our results indicate that the valley splitting of the LL is larger than the spin splitting in our samples. To our knowledge, this is the first instance where information on the sublevel structure of graphene has been obtained using infrared transmission measurements, complementing transport-[25,26] and tunneling-based [27] experiments.

We thank Cheol-Hwan Park for useful discussions. L. Z. T. and the theoretical analysis were supported by the Director, Office of Science, Office of Basic Energy Sciences, Materials Sciences and Engineering Division, U.S. Department of Energy under Contract No. DE-AC02-05CH11231. Numerical simulations were supported in part by NSF Grant No. DMR10-1006184. Computational resources were provided by NSF through TeraGrid resources at NICS and by DOE at Lawrence Berkeley National Laboratory's NERSC facility. This work has been supported in part by EuroMagNET II under EU Contract No. 228043. This work has also been supported by projects GACR Contracts No. P204/10/1020, and No. GRA/10/E006 (Eurographene-EPIGRAT), and IRMA.

*Corresponding author.

[1] A. Bostwick, F. Speck, T. Seyller, K. Horn, M. Polini, R. Asgari, A. H. MacDonald, and E. Rotenberg, Science **328**, 999 (2010).
[2] C.-F. Chen *et al.*, Nature (London) **471**, 617 (2011).
[3] L. Yang, J. Deslippe, C. H. Park, M. L. Cohen, and S. G. Louie, Phys. Rev. Lett. **103**, 186802 (2009).
[4] V. G. Kravets, A. N. Grigorenko, R. R. Nair, P. Blake, S. Anissimova, K. S. Novoselov, and A. K. Geim, Phys. Rev. B **81**, 155413 (2010).
[5] K. F. Mak, J. Shan, and T. F. Heinz, Phys. Rev. Lett. **106**, 046401 (2011).
[6] H. Suzuura and T. Ando, J. Phys. Soc. Jpn. **77**, 044703 (2008).
[7] N. Mori and T. Ando, J. Phys. Soc. Jpn., **80**, 044706 (2011).
[8] T. Ando, J. Phys. Soc. Jpn., **75**, 124701 (2006).
[9] A. Bostwick, T. Ohta, T. Seyller, K. Horn, and E. Rotenberg, Nature Phys. **3**, 36 (2006).
[10] A. C. Ferrari *et al.*, Phys. Rev. Lett. **97**, 187401 (2006).
[11] M. L. Sadowski, G. Martinez, M. Potemski, C. Berger, and W. A. deHeer, Phys. Rev. Lett. **97**, 266405 (2006).
[12] C. Berger *et al.*, J. Phys. Chem. B **108**, 19912 (2004).
[13] J. Hass, F. Varchon, J. E. Millán-Otoya, M. Sprinkle, N. Sharma, W. A. de Heer, C. Berger, P. N. First, L. Magaud, and E. H. Conrad, Phys. Rev. Lett. **100**, 125504 (2008).
[14] C. Faugeras, M. Orlita, S. Deutchlander, G. Martinez, P. Y. Yu, A. Riedel, R. Hey, and K. J. Friedland, Phys. Rev. B **80**, 073303 (2009).
[15] See Supplemental Material at http://link.aps.org/supplemental/10.1103/PhysRevLett.108.247401 for additional details of the experiment and calculation.
[16] C. H. Yang, F. M. Peeters, and W. Xu, Phys. Rev. B **82**, 075401 (2010); **82**, 205428 (2010).
[17] J. Maultzsch, S. Reich, C. Thomsen, H. Requardt, and P. Ordejón, Phys. Rev. Lett. **92**, 075501 (2004).
[18] A. Grüneis *et al.*, Phys. Rev. B **80**, 085423 (2009).
[19] M. Orlita, C. Faugeras, G. Martinez, S. A. Studenikin, and P. J. Poole, Europhys. Lett. **92**, 37002 (2010).
[20] Y. Toyozawa, M. Inoue, T. Inui, M. Okazaki, and E. Hanamura, J. Phys. Soc. Jpn. **22**, 1337 (1967).
[21] K. Yang, S. Das Sarma, and A. H. MacDonald, Phys. Rev. B **74**, 075423 (2006).
[22] K. Nomura and A. H. MacDonald, Phys. Rev. Lett. **96**, 256602 (2006).
[23] J. Alicea and M. P. A. Fisher, Phys. Rev. B **74**, 075422 (2006).
[24] J.-N. Fuchs and P. Lederer, Phys. Rev. Lett. **98**, 016803 (2007).
[25] K. Bolotin, F. Ghahari, M. D. Shulman, H. L. Stormer, and P. Kim, Nature (London) **462**, 196 (2009).
[26] X. Du, I. Skachko, F. Duerr, A. Luican, and E. Y. Andrei, Nature (London) **462**, 192 (2009).
[27] Y. Song *et al.*, Nature (London) **467**, 185 (2010).
[28] M. O. Goerbig, R. Moessner, and B. Doucot, Phys. Rev. B **74**, 161407 (2006).
[29] D. A. Abanin, P. A. Lee, and L. S. Levitov, Phys. Rev. Lett. **98**, 156801 (2007).